Composites: Part B 71 (2015) 28–39

Contents lists available at ScienceDirect

Composites: Part B

journal homepage: www.elsevier.com/locate/compositesb

Numerical experimental analysis of hybrid double lap aluminum-CFRP joints

G. Marannano, B. Zuccarello *

Università di Palermo, Dipartimento di Ingegneria Chimica, Gestionale, Informatica, Meccanica Viale delle Scienze, 90128 Palermo, Italy

ARTICLE INFO

Article history:
Received 16 August 2014
Received in revised form 18 October 2014
Accepted 18 November 2014
Available online 25 November 2014

Keywords:
A. Polymer-matrix composites (PMCs)
B. Mechanical properties
C. Finite element analysis (FEA)
E. Joints/joining

ABSTRACT

Due to their reliability and ease of assembly, both the adhesively bonded and the mechanical joints are commonly used in different fields of modern industrial design and manufacturing, to joint composite materials or composites with metals.

As it is well known, adhesively bonded joints are characterized by high stiffness and good fatigue life, although delamination phenomena localized near the free edges may limit their use, especially for applications where corrosive environments and/or moisture can lead to premature failure of the bonding. In these cases, a possible alternative is given by the well-known mechanical joints. On the contrary, these last joints (bolted, riveted) require a preliminary drilling of the elements to be joined, that may cause localized material damage and stress concentration, especially for anisotropic laminates characterized by high stress concentration factors and easy drilling damaging, with significant decrease of the load-carrying capacity of the joined elements. In order to exploit the advantages of the bonded joints and those of the mechanical joints, both industrial manufacturing and research activity have been focused recently on the so called hybrid joints, obtained by the superposition of a mechanical joint to a simple adhesively bonded joint.

In order to give a contribution to the knowledge of the mechanical behavior of hybrid bonded/riveted joints, in the present work a numerical–experimental study of bonded/riveted double-lap joints between aluminum and carbon fiber reinforced polymer (CFRP) laminates, has been carried out. It has permitted to highlight both the static and the fatigue performance of such joints obtained by using aluminum and steel rivets, as well as to known the particular damage mechanisms related also to the premature localized delamination of the CFRP laminate due to the riveting process.

1. Introduction

The increasing interest in the use of composite materials in all the fields of industrial manufacturing led the industry and many research centers toward improving the jointing processes already used for traditional metallic materials, as well as developing new techniques for joining composite materials or composite and metals. Among these, the hybrid joints obtained by the superposition of a mechanical joint with a bonded joint, are considered very interesting solutions that can allow the user to exploit the advantages of both mechanical and bonded joints.

Mechanical fasteners (using bolts, rivets, etc.) have characterized by various advantages as simple and quick disassembly without damaging, no careful preparation of the joint surface and, in generally, non sensitivity to the operative temperature and/or moisture [1–4].

The use of bonded joints, instead, permits to obtain components characterized by good stiffness, lightweight, good static and fatigue strength, thanks especially to the absence of significant notch effects on the components to be joined together.

In general, the use of hybrid bonded/bolted (or riveted) joints [5] allows the user to increase the performance of the simply adhesively bonded joints especially in the case of overload and/or significant fatigue stress [6–7].

If properly designed, the insertion of bolts and/or rivets in an adhesively bonded joint may give rise to a decrease of the maximum stress close the free edges (especially the peeling stresses) with a subsequent increase of the static and fatigue strength.

Although a significant research activity has been carried out by several authors [8], at present there are no reliable analytical models that can be used at the design stage of hybrid joints, so that a correct design is mainly based on the experimental

* Corresponding author.
E-mail address: bernardo.zuccarello@unipa.it (B. Zuccarello).

http://dx.doi.org/10.1016/j.compositesb.2014.11.025
1359-8368/

Nomenclature

E_l	longitudinal Young's modulus of the CFRP laminate	t_c	thickness of the CFPR laminate
E_{Al}	Young's modulus of the aluminum plate	t_{Al}	thickness of the aluminum adherent
$\sigma_{l,u}$	longitudinal tensile strength of the CFRP laminate	η_a	thickness of adhesive
$\sigma'_{l,u}$	longitudinal compression failure stress of the CFRP laminate	l	overlap length
		l_{min}	minimum overlap length provided by theory
$\sigma_{y,Al}$	yield stress of the aluminum	A_{riv}	transversal area of the rivet
$\sigma_{u,Al}$	tensile strength of the aluminum	G_a	shear modulus of the adhesive
$\sigma_{u,a}$	adhesive failure stress	G_{Al}	shear modulus of the aluminum
$\tau_{u,a}$	failure shear stress of the adhesive	P_R	static failure load of the joint
$\tau_{u,AL}$	failure shear stress of the aluminum plate	P_{max}	maximum fatigue loading of the joint

assessment of their mechanical behavior and of the relative performances.

The first studies accomplished by Hart-Smith [9,10] on typical aeronautical joints, have shown that, although no significant strength increment is observed respect to simply adhesively bonded joints, the hybrid joints, obtained by adding a bolting to an adhesively bonding joint, exhibit various benefits in repairing due to significant limitation of the damage propagation.

In [11] Fu Maofeng and Mallick have studied the static and fatigue behavior of hybrid single-lap joints (bolted/bonded); by an experimental investigation on the effects of different configuration of washers, the authors have observed that the performance of such hybrid joints depends significantly on the shape of the washer that influences the initial stress distributions due to the bolt tightening. Therefore, proper washer shapes that give a sufficient lateral clamping can significantly improve the mechanical performance of the joint.

Moreover, in [12] Gordon Kelly has studied the load transfer in a single-lap Al–GFRP bolted-bonded joint, by comparing the numerical results with those obtained experimentally by means of a special bolt instrumented with an electric strain gauge. It has been observed that the load transferred by the bolt increases with the thickness of the adhesive and of the adherents; on the contrary, it decreases with the increasing of both the overlap length and the elastic modulus of the adhesive.

By considering double-lap hybrid joints between GFRP elements, obtained by added rivets to simple bonded joints, in [13] Solmaz and Topkaya predict the failure mechanism and the corresponding static tensile strength by using proper numerical simulations and approximate criteria, which have also permitted to highlight that the strength of the studied hybrid joints is only slightly higher than that of the simply riveted joint (about +14%).

Sadowski et al. [14] have performed a comparative analysis of adhesively bonded, riveted and hybrid joints highlighting that, in this last case, the adding of a rivet in a bonded joint does not give rise to an appreciable increase in mechanical strength, but allows to obtain a significant increase of the energy absorption to failure, and then a significant improving of the damage tolerance and of the safety.

In [15] Ucsnik et al. have analyzed the junction between aluminum and CFRP, obtained by the superposition of a co-cured bonding joint with needle-like locking elements of the composite; by means of experimental analysis the authors have shown how the proposed innovative technique allows the user to improve the tensile strength and the energy absorption of the hybrid joint.

Jin-HweKweon et al. [16] have studied the effect of a bolt insertion on the static strength of an adhesively bonded Al–CFRP double lap joint; for the geometrical joint configuration considered, the authors have observed that the strength of hybrid joints improves only when the strength of the mechanical joint is stronger than that of the simple adhesively bonded joint.

Several studies have been carried out by Zuccarello et al. [17,18] on co-cured composite-metal joints varying the main parameters of design; in [17] they have shown that the static strength of bonded joints can be reliably predicted by using an innovative approach based on GSIFs; in [18] instead, they show that the geometrical configuration that optimize the static and fatigue performance of adhesive/bolted hybrid Al–GFRP joints, is that corresponding to the minimum overlap length provided from theory. The static and fatigue strength of such joints is given by the sum of the strength of the simply bolted joint and that of the simply bonded joint. In terms of energy absorption, the optimal configuration gives rise to a significant synergism between the simply bonded and the simply bolted joints. In this case, in fact, the energy absorption to failure is up to 3 times higher than that of simply adhesively bonded joint.

Several interesting studies on bonded and bolted joints between composite laminates and civil structures have been carried out by Ascione, Feo et al. [19–22], by considering both RC and metal beams.

In [23] Manes et al. have analyzed the fatigue behavior of riveted joints used in aeronautical applications. They have shown that the fatigue behavior is strictly influenced by the local residual stress fields left very near to the holes during riveting manufacturing operations; using the literature fatigue data of Al8090-T81 and the Crossland multiaxial fatigue criterion, the influence of the riveting parameters on the fatigue strength is evaluated for optimization purposes.

Finally, numerical studies, carried out in ANSYS APDL environment with explicit solver, have been performed by several authors [14,23] in order to verify the structural integrity of the hybrid joint after the riveting process.

Several studies reported in literature [24–26] show, in fact, that the radial deformation of the rivet can led to significant compressive residual stresses around the hole, with consequential interlaminar damage of the composite laminate.

In order to give a contribution to the design of hybrid bonded/riveted joints between aluminum and CFRP laminates, in the following a systematic numerical–experimental study of both the static and the fatigue performance, has been carried out. Also, by considering hybrid joints obtained by using aluminum and steel rivets, the particular damage mechanisms related to the premature localized delamination of the laminates due to the riveting process, have been studied.

2. Materials and geometry of analyzed joints

2.1. Materials

In the present paper double-lap joints between aluminum and CFRP components are considered. This configuration is widely used

in both aeronautical and automotive field, where these materials are adopted for realizing components and structures characterized by high mechanical performance and lightweightness.

In particular, a quasi-isotropic CFRP $[0/\pm45/90]_s$ composite laminate made of 8 unidirectional layers has been considered. For the composite manufacturing, a stitched carbon fabric (unit weight of 200 g/m^2) and a SX-10 epoxy resin [27] having Young modulus $E_a = 3$ GPa, Poisson ratio $\nu_a = 0.39$, tensile strength $\sigma_{u,a} = 60$ MPa, shear strength $\tau_{u,a} = 30$ MPa, have been used. The laminate has been prepared by hand lay-up process using vacuum bag technique, and it has been successively cured at 80 °C for 1 h.

Such a laminate lay-up has been selected because it permits to obtain good strength characteristics for both bonded joints and mechanical joints. In fact, the external layers aligned with the applied load allows to reach the maximum performance of the adhesively bonded joint, whereas, according to the classical laminate theory (CLT), the internal layers oriented at ±45° allows to obtain a good stiffness and shear strength of the laminate, that is necessary condition to avoid a premature shear failure of the mechanical joint [13]. The main physical characteristics of the CFRP laminate are shown in Table 1.

According to ASTM D3039 [28], the main mechanical characteristics of the composite laminate CFRP have been determined by several tensile tests, performed on rectangular specimens with aluminum tabs (see Fig. 1A).

The tests have been carried out by using a MTS 810 servo-hydraulic testing machine with load cell of 100 kN and crosshead speed of 1 mm/min. The axial strain of the specimen is acquired by a MTS extensometer (model 832.12c-20), with base length of 25 mm.

The experimental tests have shown that the composite exhibits a linear elastic behavior until failure. The longitudinal Young's modulus is equal to $E_l = 49$ GPa and the longitudinal tensile strength $\sigma_{l,u} = 418$ MPa. The failure is characterized by XGM debonding mode [28], as shown in Fig. 1B. Through Micromechanics and CLT a compressive strength $\sigma'_{l,u} = 515$ MPa has been also computed.

The aluminum adherent is made by a 6xxx serie aluminum alloy, classified as UNI EN AW-6082-T6 (Anticorodal) alloy, that can be strengthened by heat treatment (precipitation hardening), and is characterized by the presence of elements as silicon and magnesium. These alloys are generally less strong than the 2xxx and 7xxx series, but have good formability and are weldability. According to the classification, the mechanical properties of such aluminum alloy are: Young's modulus $E_{Al} = 68$ GPa, yield stress $\sigma_{y,Al} = 295$ MPa, tensile strength $\sigma_{u,Al} = 316$ MPa.

The simple adhesively bonded joint and the hybrid double-lap joint between CFRP and aluminum plate have been bonded together by means of ISOBOND SR 1170 high performance epoxy resin produced by Sicomin Epoxy Systems. It has a shear modulus $G_a = 1100$ MPa and a shear strength $\tau_r = 31$ MPa.

For the riveting process, aluminum and steel rivets with diameter $d = 4$ mm, length $L = 14$ mm and outer diameter $D = 8$ mm (see Fig. 2), are used. This kind of rivet is suitable for the junction of superimposed elements with overall thickness ranging from 8.5 to 10.5 mm.

Table 1
Characteristics of the CFRP composite laminate.

	Fibers	Resin	Composite
Weight ratios (%)	0.68	0.32	–
Density (g/cm^3)	1.75	1.2	1.53
Volumetric content (%)	0.59	0.41	–

2.2. Geometry of the joint

According to the bonded joints theory [29–33], in order to avoid strongly asymmetric shear and peeling stress distributions at the adhesive–adherents interface, the thickness of the adherents must be chosen properly in such a way to realize quite balanced joints, i.e. joints in which the stiffness of the interior adherent is equal to the sum of the stiffness of the external adherents. An unbalanced joint in fact leads to an increase of stresses on the attach edge of the more yielding adherent [29–33] and therefore, for fixed work conditions, it shows a lower strength than a balanced joint, regardless of the particular load direction (tensile or compression).

In the examined case of CFRP external adherents with thickness $t_c = 2$ mm, the balanced condition requires a thickness of the internal aluminum alloy adherent $t_{Al} = 3$ mm. Taking into account that the strength of the aluminum alloy is lower than that of composites, as well as the stress concentration around the holes, in order to joint elements with comparable strength, a thickness $t_{Al} = 4$ mm has been adopted.

Moreover, the overlap length "l" has been fixed in accordance with the approach used in the aeronautical field, in which it is about twice the minimum overlap length (l_{min}) provided by the Hart-Smith theory [32] (see Eq. (1)):

$$l = 2l_{min} = 2\left(\frac{\sigma_{l,u}t_c}{\tau_{u,a}} + \frac{2}{\beta}\right) = 90 \text{ mm} \tag{1}$$

where

$$\beta = \frac{\lambda}{\alpha} = \frac{\sqrt{\frac{2G_a}{\eta_a E_l t_c}\left(\frac{1+S}{2S}\right)}}{\sqrt{1 + \frac{G_a}{\eta_a}\left(\frac{t_{Al}}{6G_{Al}} + \frac{t_c}{3G_{lt}}\right)}} = 0.168 \tag{2}$$

Fig. 3 shows the geometry of the simple adhesively bonded joints. Fig. 4 shows, instead, the geometry of the simple riveted and hybrid joints.

In the experimental work, the bonding of both the simply bonded and hybrid joints has been carried out by using ISOBOND SR 1170 epoxy adhesive with a thickness $\eta_a = 0.4$ mm.

All the joint type considered have been tested by using 4–5 specimens, so that each determined parameter has been characterized by the corresponding mean value and standard deviation.

3. Static analysis

In order to determine the tensile strength of the analyzed joints as well as to study the particular damage mechanisms under static stress, the specimens have been subjected to proper tensile tests performed by using a MTS 810 servo-hydraulic testing machine.

According to ASTM standard [34], all the experimental tests have been carried out under a constant crosshead speed of 1 mm/min.

3.1. Simple bonded joints (SB) and simple riveted joints (SR)

Fig. 5 shows the experimental data obtained by tensile tests on simple adhesively bonded joints (SB, see Fig. 5A) and simple riveted joints (SR, see Fig. 5B) with aluminum (SR_AL) and steel (SR_STEEL) rivets.

From Fig. 5A it is possible to observe that in practice the simple adhesively bonded joints show a linear behavior until failure. The analysis of the corresponding fracture surface (see Fig. 6A) shows that the failure of the joint is caused by the adhesive failure at the interface with the aluminum alloy adherent; in accordance with the theory, the failure propagates from the attach edge of the more compliant adherent, that is the external CFRP adherent.

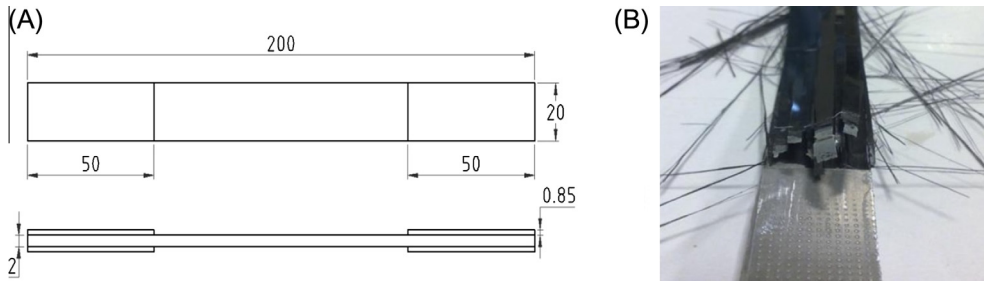

Fig. 1. (A) Dimensions of the specimens used for the experimental characterization of the CFRP composite laminate and (B) detail of static tensile failure mode.

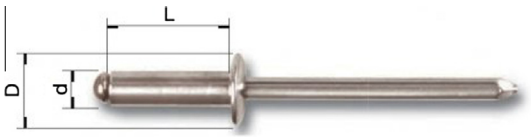

Fig. 2. Characteristic dimensions of the aluminum and steel rivets used for the analyzed joints.

Fig. 5B shows instead that the simple riveted (SR) specimens, with aluminum and steel rivets, initially exhibit a linear behavior, followed by a successive elasto-plastic phase. Then it follows a final phase characterized by a load decrease, up to the complete failure of the joint.

In particular, it is possible to observe that both the specimens (with aluminum and steel rivets) exhibit in practice the same stiffness in the elastic and elasto-plastic phases, although the loads of the linearity deviation are different (respectively, about 3 kN and 6 kN for aluminum and steel rivets) as well as different are the tensile strength P_R (about 5 kN and 8.5 kN for specimens with aluminum and steel rivets, respectively).

Obviously, the linearity deviation corresponds to the transition from the initial condition in which the load is transmitted exclusively by friction, due to the preload of the rivet, at the secondary condition in which part of the load is transmitted through shear stresses on the rivet, with bearing stress of the material near the hole edge.

In particular, the specimens with steel rivets exhibits a failure load of about 70% higher than that of the specimens with aluminum rivets.

The experimental tests of the simply riveted specimens (with steel rivets) show that the failure of the joint is caused by the flexural deformation of the rivet (see Fig. 6B), followed by a significant localized damage of the composite material around the hole and the final pull-out of the rivet.

Considering instead the simple riveted joint with aluminum rivet, it has been observed that the final failure of the joint is caused by the shear failure of the rivet without significant bending

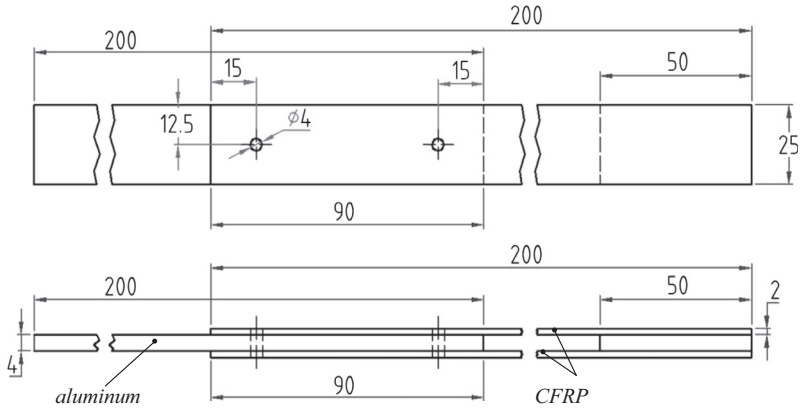

Fig. 3. Geometry of the simply adhesively bonded joints.

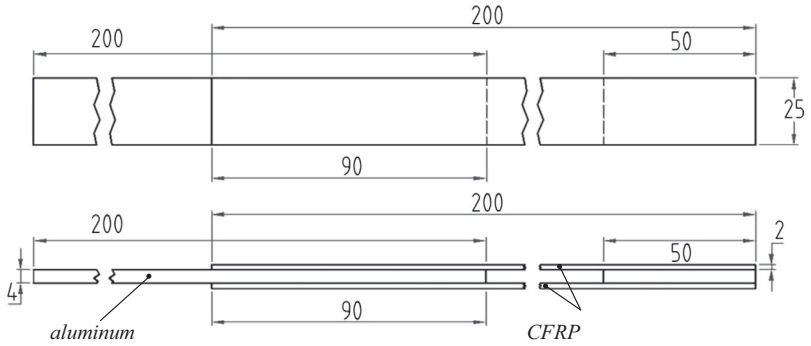

Fig. 4. Geometry of the simply riveted and hybrid joints.

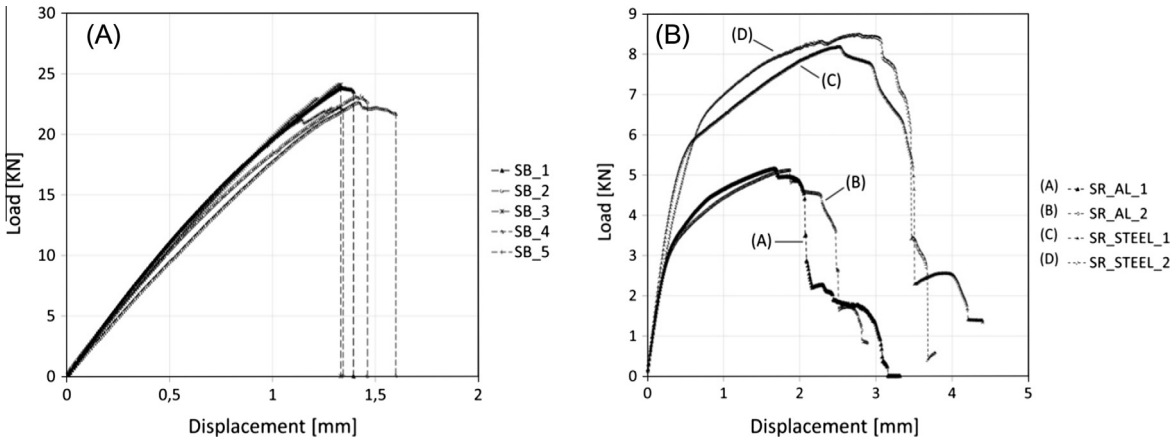

Fig. 5. Tensile test results for simply adhesively bonded joints (A) and simply riveted joints (B).

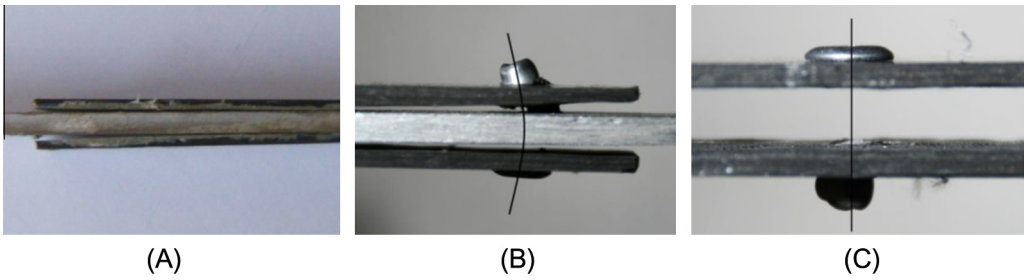

Fig. 6. Failure mode of (A) simply adhesively bonded joints, simply riveted joints (B) with steel rivets and (C) aluminum rivets.

effects or pull-out phenomena (see Fig. 6C). In this case, no significant damage of the composite and aluminum adherents, is observed.

The failure load of the joint with aluminum rivets $P_{R(SR\_Al)}$ corresponds to the ultimate shear load of the rivets. In fact, in accordance with the experimental results, it follows:

$$P_{R(SR\_Al)} = 2\tau_{u,Al}A_{riv} = 2 \cdot 200 \cdot 12.56 \approx 5 \text{ kN} \quad (3)$$

The failure load of the joints with steel rivets $P_{R(SR\_Steel)}$ corresponds, instead, to the bearing strength (compression) of the composite adherent. In fact, in this case the failure load is:

$$P_{R(SR\_Steel)} = \sigma'_{l,u}A_r = 515 \cdot 4 \cdot 2 \cdot 2 \cdot \approx 8.25 \text{ kN} \quad (4)$$

3.2. Hybrid joints (with aluminum and steel rivets)

The load–displacement curves obtained by tensile tests of the hybrid joints with aluminum rivets (HYBRID_AL) are shown in Fig. 7A. It is seen a quasi-linear behavior of the joint up to a relatively high tensile loads (near the failure load), followed by a sub-horizontal non-linear trend (elasto–plastic) and a final abrupt failure. In practice, the experimental evidence shows that the progressive failure of the adhesive layer is followed by a gradual load transfer to the rivet (area with non-linear behavior due to the variation of the stiffness) and a subsequent sudden failure of the joint that always occurs as a result of the shear failure of the rivet; the

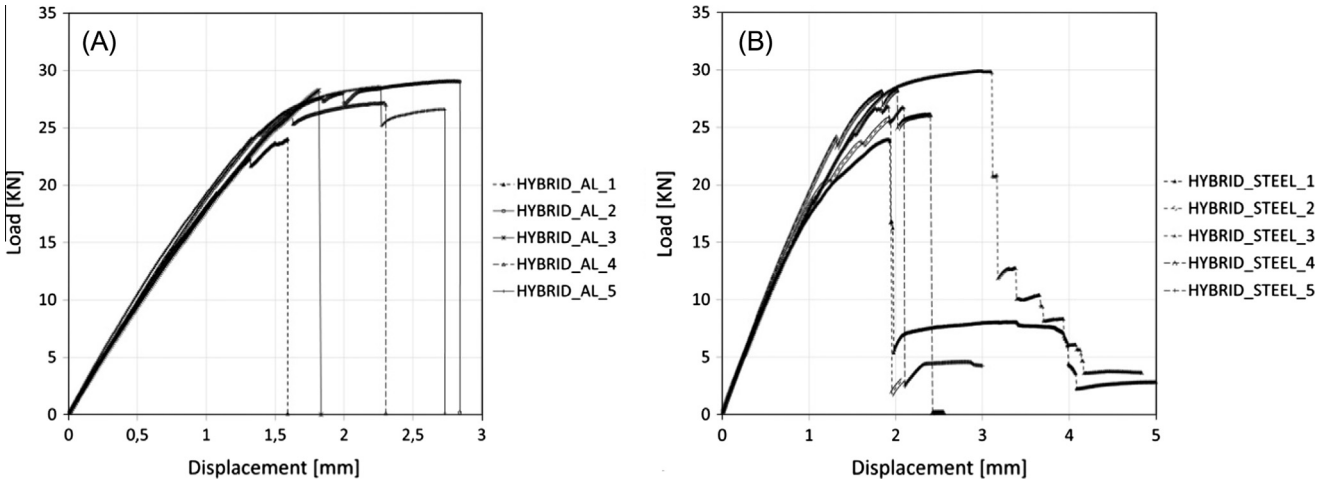

Fig. 7. Tensile test results for hybrid joints with (A) aluminum rivets and (B) steel rivets.

final damage of the joint occurs abruptly because the rivet is not able to bear the applied load after the failure of the adhesive layer.

A similar behavior is exhibited by the hybrid joints with steel rivets (HYBRID_STEEL), until the failure load is reached (see Fig. 7B). In detail, a first elastic phase followed by an elasto–plastic phase that stop at a failure tensile load similar to that of the hybrid joint with aluminum rivet, are again observed. Unlike the case of the hybrid joints with aluminum rivets, when the failure load is reached, a partial drop-down of the load towards values equal to 15–20% of the failure load is now observed. Also, the failure strains are significantly higher than those recorded for the hybrid specimens with aluminum rivets (higher energy absorption to failure).

After the joint failure, the analysis of the failure surface of the hybrid joints with aluminum rivet shows that, due to the discontinuity introduced by the hole, the portion of the first layer (aligned with the axis of the joint) of the CFRP laminate included between the two rivets, remains bonded to the aluminum plate (see Fig. 8A). Moreover, a net-tension failure mode is observed in the transversal section corresponding to one of the two rivets. In general, the heads of the rivet do not cause any significant deformation in the CFRP laminate (see Fig. 8B that shows the zone of the CFRP laminate near the hole, as it appear after failure).

The post-failure analysis of the damage process of the hybrid joint with steel rivets, instead, shows that the joint failure follows the bending of the rivet and its pull-out from the composite laminate, that occurs after the brittle fracture of the adhesive.

Due to the higher shear strength of the steel rivet, the CFRP laminate is now locally deformed and damaged (see Fig. 9A and B), like already observed in the case of simple riveted joint with steel rivets (see also Fig. 6B).

Therefore, by comparing the performance of the hybrid joints (Fig. 7) with that of the corresponding simple adhesively bonded joints and simple riveted joints (Fig. 5), it can be stated that:

(1) the failure load of the hybrid joints with aluminum rivets is equal to the sum of the failure loads of the two corresponding simply bonded and simply riveted joints;
(2) with respect the simply adhesively bonded joint, the increase of the failure load of the hybrid joint with steel rivets is equal to about 5 kN, corresponding to about 60% the failure load of the simple riveted joints.

In other words, in the case of the hybrid joint with aluminum rivets, the geometry and the mechanical characteristics of the coexistent joinings determine that the applied load is distributed between the adhesive and the rivet in such a way that at the incipient joint failure the actual load supported by each junction (bonded, riveted), is close to the corresponding strength. Consequently, when the failure of the adhesive layer starts, the load supported by the rivet is about equal to its shear failure load, so that the final failure of the joint occurs abruptly (see Fig. 7A) due to the simultaneous damage of the adhesive layer and the rivets.

This optimal result does not occur for the hybrid joint with steel rivets because in this case when the failure of the adhesive layer starts, the load supported by the rivet is the same that in the case of aluminum rivet (5 kN), but it is significantly lower (about 60%) than the corresponding failure load of the rivet (about 8.25 kN, see Fig. 5B). Therefore, in this case the adhesive failure is followed by the partial drop-down of the load with final average value corresponding to the failure load of the steel rivet, as shown in Fig. 7B.

Like in [18], by defining the percentage efficiency of the hybrid joint ($e_{\%}$) as the ratio of the failure load of the hybrid joint and the sum of the failure loads of the corresponding simple junctions (simply bonded and simply riveted), it can be observed that the hybrid joints with aluminum rivets have an efficiency of 100% whereas the hybrid joints with steel rivets have an efficiency of about 90%. In fact:

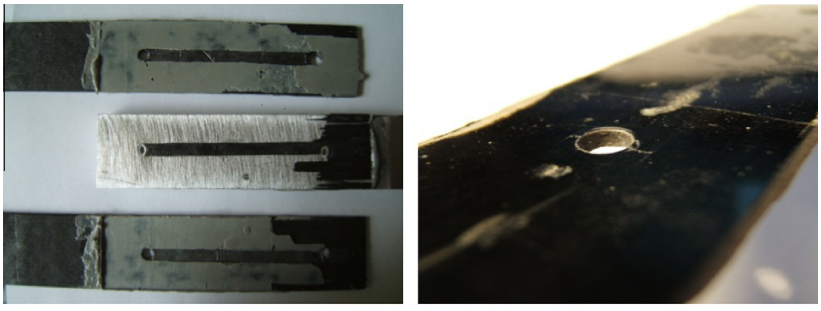

Fig. 8. (A) Damaged surface of the hybrid specimens with aluminum rivets and (B) absence of damage of the CFRP composite laminate, near the hole.

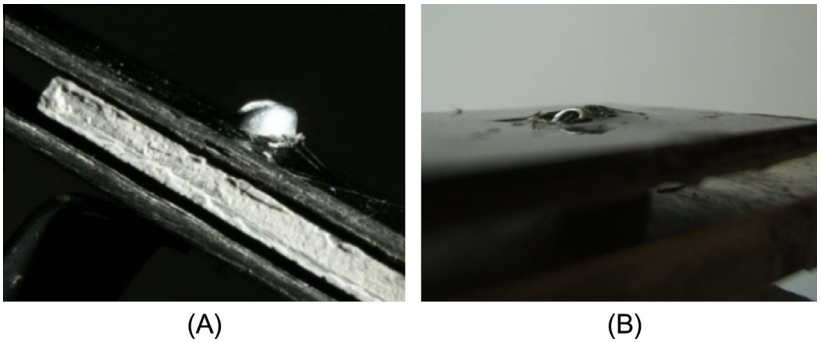

Fig. 9. (A) Damaged surface of the hybrid joint with steel rivets and (B) damage of the CFRP near the hole after the pull-out of the rivet.

$$e_{\%}(aluminum) = 100\frac{P_{R,Hybrid}}{P_{R,bonded} + P_{R,riveted}} = 100\frac{28\text{kN}}{23\text{kN} + 5\text{kN}} = 100\% \quad (5)$$

$$e_{\%}(steel) = 100\frac{P_{R,Hybrid}}{P_{R,bonded} + P_{R,riveted}} = 100\frac{28\text{kN}}{23\text{kN} + 8\text{kN}} = 90\% \quad (6)$$

In order to allow a quick comparison of the above described results, Fig. 10A and B shows respectively the average values of the tensile strength and the stiffness of the different junctions examined.

From Fig. 10A, it is seen that for the material couple analyzed, the insertion of rivets on a simply adhesively bonded joint allows to obtain an appreciable increase of the tensile strength. In the presence of the brittle adhesive used in this work, this result is mainly due to the preload of the rivet that reduces the magnitudes of the maximum peeling stress on the adhesive layer, near the free edges [35]. Moreover, the partial load transmission through the rivet gives rise to a decrease of the maximum shear stress in the adhesive layer, near the free edges, where the adhesive failure always starts.

In absolute terms, with respect to the mechanical performances of the simply adhesively bonded joint, the increase of the load carrying capacity of the hybrid joints is however rather limited (about 20%) due to the low strength of the aluminum rivets and of the local damage of the CFRP laminate (steel rivets). Better results could be obtained by substituting the rivets with proper bolts [18] that permit to obtain higher preload values, with a consequent higher reduction of the peeling stresses (near the free edges) as well as of the bearing stresses on the composite adherent (near the hole edges). In fact, due to the higher preload, for a fixed applied tensile load, a higher rate of the external load is transmitted by friction and this permits to avoid the pull-out of the mechanical element that is the main cause of the failure of the hybrid joint (bonded and riveted).

From Fig. 10B, it can be observed that in the hybrid joints the rivets insertion do not cause an appreciable decrease of the stiffness, with respect to that of the simple adhesively bonded joints. As already seen for the simply adhesively bonded joints, the hybrid joints have a stiffness about twice that of the simply riveted joints.

Finally, Fig. 11 shows the energy absorption to failure for all the various joints examined. From this figure it is possible to observe that, in addition to the increase of the overall static strength, the hybrid joints exhibit, if compared to the simply adhesively bonded joints, an appreciable increase of the energy absorption to failure, and then a significant increment of the damage tolerance.

In more detail, the hybrid joints with aluminum rivets exhibit a synergistic effect, i.e. an energy absorption to failure equal to twice that of the simple adhesively bonded joints and equal to about four times that of the simple riveted joints.

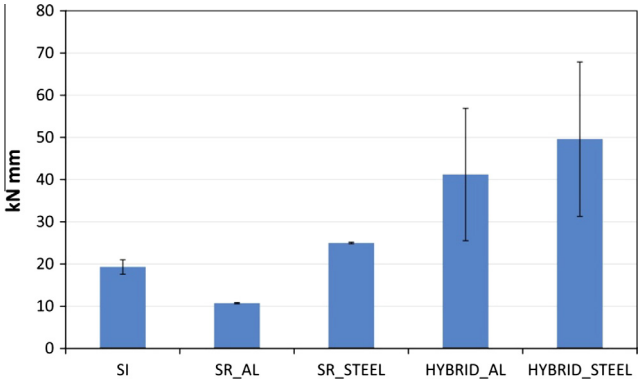

Fig. 11. Average energy absorption to failure for all the different double-lap joints analyzed.

The observed synergism is still more marked in the hybrid joints with steel rivets: in fact, they exhibit an energy absorption to failure equal to about 2.5 times of the simple adhesively bonded joints and equal to about 5 times that of the simple riveted joints.

Therefore, it is possible to state that the greater advantages of the examined hybrid joints are in terms of static damage tolerance (if compared to the simply adhesively bonded joints and the simply riveted joints); it follows the tensile strength, with joint efficiencies ranging from 90% (steel rivets) to 100% (aluminum rivets), and the stiffness that, however, remains almost equal to that of the simple adhesively bonded joints.

4. Fatigue tests

Although interesting works on the fatigue strength of adhesive, riveted and hybrid joints are reported in the literature [36–38] by considering the effects of mean stress and the load ratio, as well as the possibility to predict the fatigue life by using numerical approaches based on the so-called cohesive Zone Model (CZM), the study of the fatigue performance of the analyzed joints needs a direct experimental analysis. In fact, in the presence of variable loads the mechanical performance of a joint are closely related to the peculiar behavior of the adhesive, the particular geometrical configuration of the joint and the actual preload of the rivet.

In order to evaluate the fatigue strength of the hybrid joints considered in the present work, as well as to highlight their advantages with respect to the simply adhesively bonded joints, various fatigue tests have been carried out by applying a sinusoidal load to the simply adhesively bonded joints and to the hybrid joints (with aluminum and steel rivets). In detail, a MTS servo-hydraulic fatigue

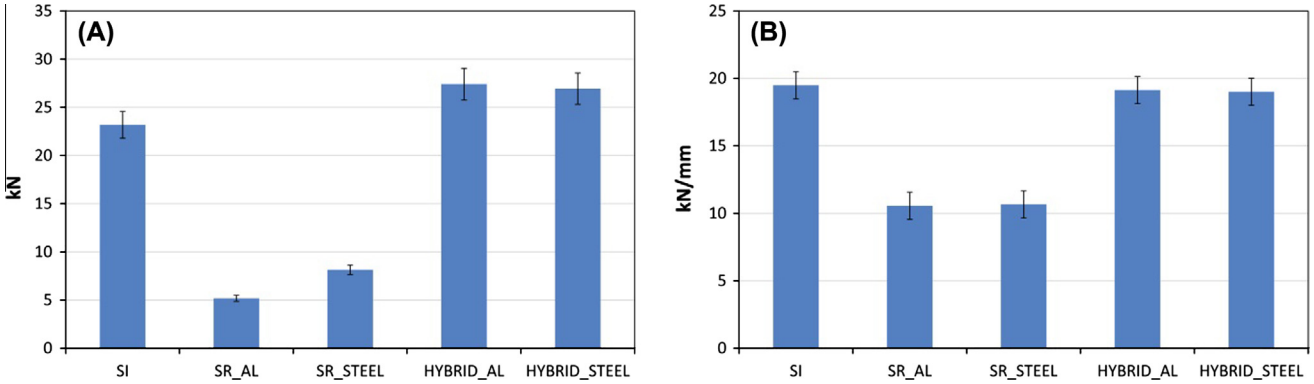

Fig. 10. (A) Average tensile failure load and (B) average stiffness of the joints analyzed.

testing machine with a load cell of 100 kN, load ratio of $R = 0.1$ (traction–traction) and load frequency equal to 10 Hz, have been used. In accordance with the literature [8], such a load frequency does not lead to heating of the CFRP due to mechanical hysteresis.

For each examined joint, the fatigue load levels have been chosen by taking into account the corresponding ultimate load determined through the static tests. The tests have been performed in "load control" mode, with maximum load value ranging from 40% to 70% the ultimate static load.

Fig. 12 shows the results obtained by the fatigue tests, i.e. the Wöhler curves of the various analyzed joints.

Similarly to composite laminates [39,40] and simply adhesively bonded joints between metal elements [31–33], the fatigue curves reported in Fig. 12 shows that the fatigue behavior of the analyzed joints can be described by the following analytical function:

$$P_{max} = a + bLog(N) \tag{7}$$

The best fitting procedure of the experimental results, in the range 10^3–10^6 cycles, allows to evaluate the values of the characteristics parameters a and b for the three types of examined joints (see Table 2).In detail, the examination of the fatigue curves shows in Fig. 12, reveals that the superposition of rivets to a simple adhesively bonded joints leads to significant increases of the fatigue life. The results, however, are different for aluminum and steel rivets respectively.

In more detail, the fatigue curve of the hybrid joint with steel rivet is almost parallel to that of the simply adhesively bonded joint and, therefore, regardless the number of fatigue cycles, the increase of the fatigue strength is constant and equal to about 3 kN.

In relative terms, the benefits increase from about 20% at 10^3 cycles (low cycles fatigue) to about 45% at 10^6 cycles (high cycles fatigue). Therefore, with respect to the simply adhesively bonded joints, it is possible to state that the fatigue performances of the hybrid joints with steel rivet improves further by moving from static loading (+20%) to high cycles fatigue loading (+45%).

Opposite results are instead obtained for the hybrid joints with aluminum rivets; in fact, Fig. 12 shows that the fatigue curve of such joints has a higher slope compared to that of the simply adhesively bonded joints and, therefore, the improvement of the fatigue performance decreases by moving from static loading to high cycles fatigue. In detail, the increase of the fatigue strength is equal to about 2 kN for low cycles fatigue (about +10% at 10^3 cycles) and tends to zero for a high cycles fatigue (10^6 cycles). Therefore, in terms of fatigue strength, with respect to the simply adhesively bonded joints, the advantages of the hybrid joints with aluminum rivet decrease again by passing from static loading (+20%) to the high cycles fatigue (0%, at 10^6 cycles).

Table 2
Fatigue constants for the simply bonded and hybrid joints with aluminum and steel rivets.

Fatigue constants	Double-lap joint		
	SB	HYBRID_AL	HYBRID_STEEL
a	29,100	33,151	32,922
b	−1620	−1901	−1715

These results are easily understood by considering the experimental evidence that show how under fatigue loading, the failure of the simple adhesively bonded joints occurs abruptly due to the damage of the adhesive caused by the crack growth at the aluminum–adhesive interface. A similar failure mode it has been observed for the hybrid joints with aluminum rivets, where the damage of the adhesive at the aluminum–adhesive interface follows the abruptly load transfer to the rivets with a consequent shear failure of the same element.

Regarding to the hybrid joints with steel rivets, instead, it has been observed that the failure involves two distinct phases; the progressive failure of the bonding interface followed by the bearing failure of the composite adherent with subsequent pull-out of the rivets from the CFRP laminate.

Unlike hybrid joints with aluminum rivets, in the case of high cycles fatigue, the fatigue life of the joints with steel rivets is in part spent for the damage of the adhesive bonding (nucleation and propagation of the aluminum–adhesive interface crack) and in part spent for the rivet damage and, especially, for the composite bearing failure. In detail, the experimental tests have shown that for low fatigue loads (less than 50% the static failure load), a relevant damage of the composite adherent occurs (see Fig. 13A), whereas for fatigue loads higher equal or higher than 50% of the static failure load, no significant damage for the composite adherent is observed (Fig. 13B).

The fatigue tests with low load value, in fact, are characterized by a slower growth of the adhesive–aluminum interface crack with a more gradual transfer of the load on the rivet, before the final failure of the joint. This causes a considerable fatigue damage of the CFRP laminate near the hole edge. For fatigue loads that exceed

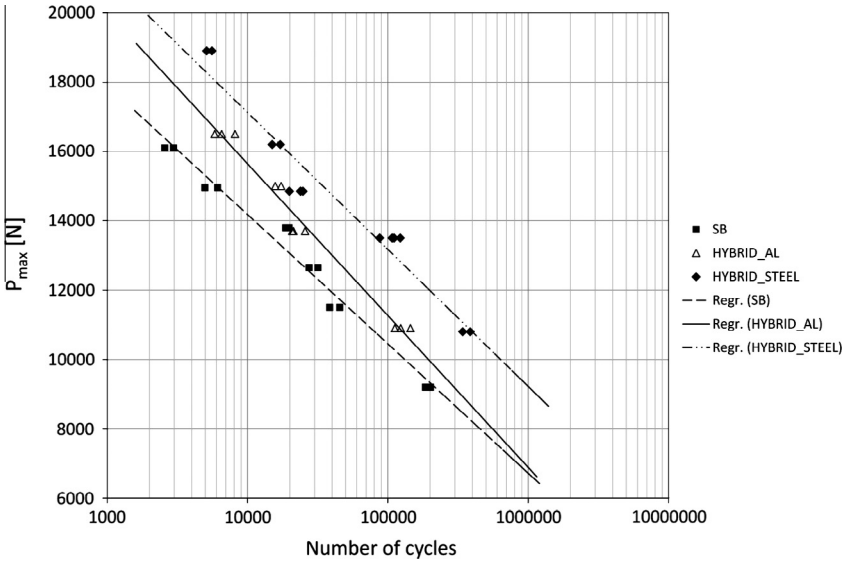

Fig. 12. Wöhler curves for the various joints analyzed.

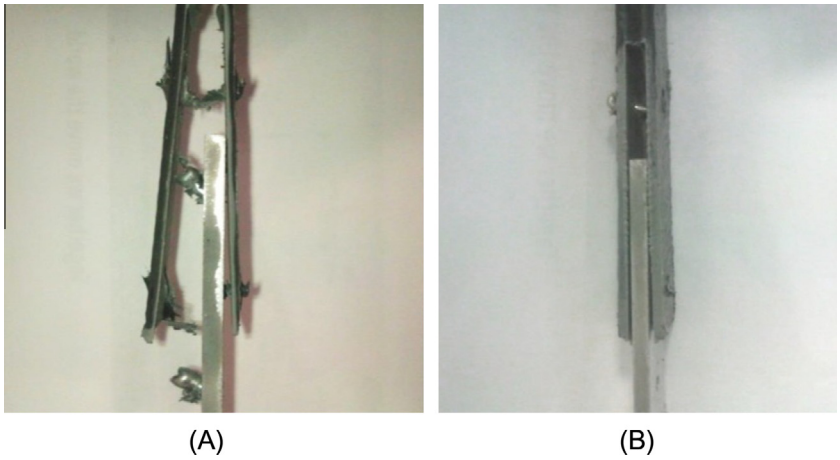

Fig. 13. (A) Fatigue damage of the hybrid joints with steel rivets for maximum applied load less than and (B) higher than 50% of the static failure load.

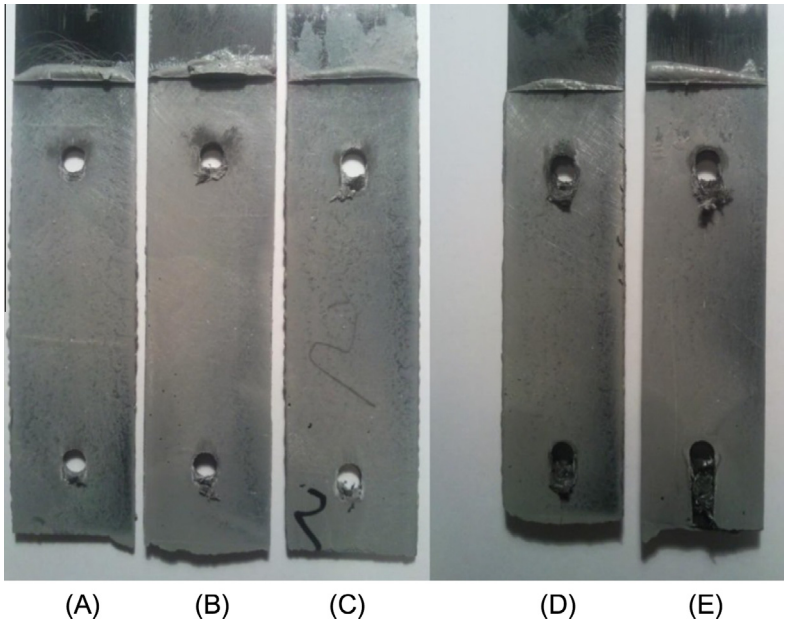

Fig. 14. Typical fatigue damage of the CFRP near the hole edge for the hybrid joints with steel rivets and P_{max} equal to (A) 70%, (B) 60%, (C) 55%, (D) 50%, (E) 40% of the static failure load.

50% the static failure load, instead, the fatigue damage of the holes on the CFRP adherent is very small and comparable with that observed previously in the static case.

As an example, Fig. 14 shows the fatigue damage of the CFRP for maximum applied load equal to 70% (A), 60% (B), 55% (C), 50% (D) and 40% (E) of the static tensile strength.

In terms of fatigue life, Fig. 12 shows that if the maximum applied load (P_{max}) varies between 40% and 70% of the static failure load (P_R), moving from simple adhesively bonded joints to hybrid joints with steel rivets, the number of cycles to failure increases from 5 to 6 times. As an example, for $P_{max} = 70\%\ P_R$ the number of cycles to failure increases from 1000 to 6000 cycles, whereas for $P_{max} = 40\%\ P_R$ the number of cycles to failure increases from $2 \cdot 10^5$ a 10^6 cycles.

By moving from simply adhesively bonded joints to hybrid joints with aluminum rivets, more limited advantages are instead observed. As an example, for $P_{max} = 40\%\ P_R$ it does not occur any increase in the number of cycles to failure, whereas for $P_{max} = 70\%\ P_R$ the life of the joint increases from 1000 to 3000 cycles.

In conclusion, by taking into account that the above exposed experimental analysis has shown that:

(1) under static load conditions the performance of the hybrid joints with steel rivets is comparable with that obtained by using aluminum rivets;
(2) under fatigue loading the performance of the hybrid joints with steel rivets is significantly higher than that obtained with aluminum rivets;
(3) due to the aluminum–CFRP galvanic couple, the use of aluminum rivets can gives rise to significant corrosion phenomena near the hole edges where the carbon fibers may be in direct contact with the rivet;

it follows that the use of aluminum rivets are not advisable, whereas the use of steel rivets is certainly the best solution for the realization of hybrid joints between aluminum and CFRP elements.

5. Numerical simulation of the riveting process

In order to verify possible damage of the composite laminate due to the riveting process, several numerical simulations of the riveting process have been carried out by using the ANSYS

Parametric Design Language (APDL) environment and the explicit solver applied to parametric models of the hybrid joints with steel and aluminum rivets. This approach has already been used and validated by other authors for similar joint types [14,18].

In particular, the numerical analyses have been carried out by using three-dimensional models of the hybrid double-lap joint in which the quasi-isotropic CFRP $[0/\pm45/90]_s$ composite laminate made of 8 unidirectional layers, has been modeled layer by layer. In more detail, the numerical models are discretized by means of 8-node SOLID 164 elements, properly optimized for the 3-D modeling of solid structures. To reduce the computing time, the internal pin of the rivet has been considered as a rigid body, whereas the external body of the rivet has been modeled by defining a bilinear isotropic hardening material model (*TB*, *BISO*) in which the stress-strain curve start at the origin with slope equal to the elastic modulus of the material; at the specified yield stress, the curve continues along the second slope defined by the tangent modulus.

Table 3 shows the parameters used to define the mechanical properties of steel and aluminum elements used in the numerical simulation of the riveting process.

The mechanical properties of each orthotropic lamina that constitutes the CFRP laminate, have been defined by means of a local coordinate system. The adjacent laminae have been defined as independent elements, separated at the interface with proper overlapping nodes.

Due to their axisymmetry, the rivets have been modeled by revolved boss/base operation. Tie break surface-to-surface contacts (TSTS) elements have been located at the interface between the composite laminae and between the composite adherents and the aluminum plate, to define the possible failure surfaces by applying the maximum stress criterion to normal and shear stresses acting on the surfaces of the composite laminae and on the bonded surface of the metal adherend.

An additional contact types NTS (Node-To-Surface contact) have been defined in order to model the contact between the outer surface of the deformable body of the rivet and the inner surface of the hole.

After the definition of the parts of the dynamic module, the riveting process has been simulated by imposing to the rivet pin a displacement of 1.5 mm/s.

Fig. 15A shows a detail of the discretization of the hybrid joint model, with steel rivet at the start point of the numerical simulation of the riveting process; Fig. 15B shows instead the forming of the rivet counterhead at the end of the numerical simulation.

Fig. 16A shows, instead, the extension of the interlaminar damage predicted by the simulation in the CFRP laminate (with steel rivet) at the end of the riveting process.

Fig. 16B shows a detail of the area near the rivet head, that permit to observe the delamination phenomena highlighted by the relative displacement of the free edges of the first five laminae of the CFRP adherent.

Finally, Fig. 17 shows the extension of the interlaminar damage (colored zones) for a longitudinal section of the hybrid joint with steel rivet (Fig. 17A) and aluminum rivet (Fig. 17B).

From Fig. 17A it is possible to observe a significant interlaminar damage of the CFRP laminate near the head side of the steel rivet in

Table 3
Numerical parameters used to define the elastic-plastic properties of the rivets.

	Steel rivet	Aluminum rivet
Density (kg/mm^3)	$8.75 * 10^{-6}$	$2.75 * 10^{-6}$
Young's modulus (GPa)	210	69
Poisson's ratio	0.28	0.33
Yield stress (MPa)	475	230
Tangent modulus (MPa)	20	20

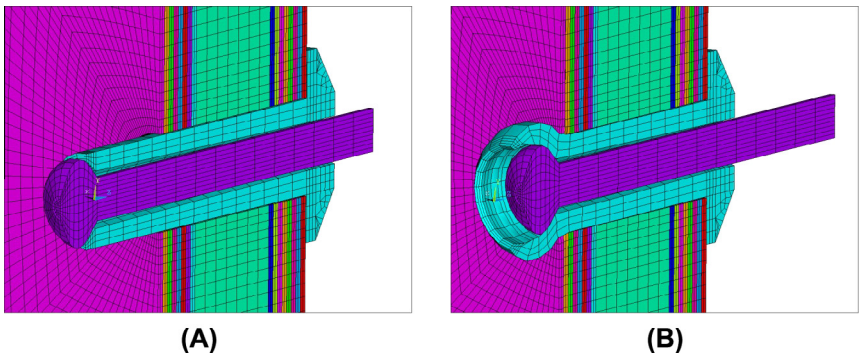

Fig. 15. (A) Detail of the FEM model at the beginning of the riveting process and (B) at the end of the riveting process.

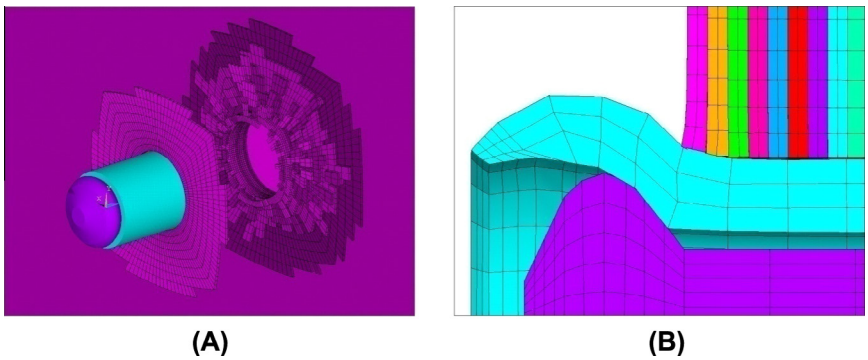

Fig. 16. (A) Extension of interlaminar damage as a result of the riveting process with steel rivet and (B) detail of the delaminated area around the hole.

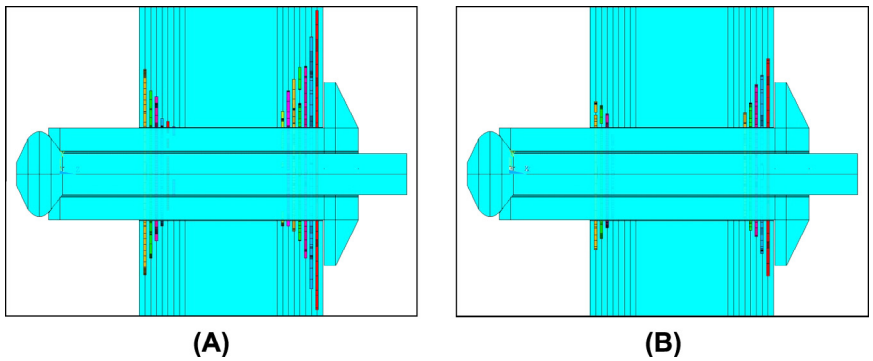

Fig. 17. Interlaminar damage zone on the CFRP adherents as a result of the simulation of the riveting process using steel rivet (A) and aluminum rivet (B).

the annular zone around the hole. Near the external surface of the laminate the delamination have an extension equal to about the hole diameter. In particular, it is possible to observe a significant delamination at the interface between the first lamina (oriented at 0°) and the second lamina (oriented at +45°). Moving from the outer surface of the CFRP towards the inner surface, it is observed a progressive reduction of the damage that tends to zero at the composite–aluminum interface. Also, the interlaminar damage of the CFRP adherent near the counterhead rivet side is significantly less than that near the head rivet side.

Moreover, the extension of the interlaminar damage caused by the use of the steel rivet (Fig. 17A) is more than that due to the aluminum rivet (see Fig. 17B). In detail, in the case of aluminum rivet the maximum delamination extension is equal to about 0.7 times the hole diameter, and it occurs at the rivet head side, always at the interface between the two outer laminae.

Finally, the higher extension of the interlaminar damage on the hybrid joint with steel rivet, corroborates the lower static joint efficiency observed experimentally, with respect to the hybrid joint with aluminum rivet.

In fact, in accordance with the experimental evidence, the CFRP delamination near the hole edge (caused by riveting process) reduces not only the local effects of the preload, but also the static bearing strength of the joint and leads to the premature pull-out of the rivet, as observed in the static tests (see Fig. 9A).

Such an interlaminar delamination justified the higher CFRP fatigue damage around the hole for lower operating loads, i.e. for high cycles fatigue (see Fig. 12A), due to the stable propagation of the delamination started by the riveting process.

6. Conclusions

In this paper, by a systematic experimental study of double-lap joints between an AW 6082 T6 aluminum and a quasi-isotropic CFRP laminate $[0/\pm45/90]_s$, it has been demonstrated that the introduction of steel or aluminum rivets on an adhesively bonded joint having overlap length equal to twice the minimum size recommended by the theory (configuration typically used in the aeronautical field), allows to improve the static strength and, especially, the fatigue performances. The mechanical strength increment is included between 20% for static loading, to about 45% for high cycles fatigue.

Moreover, the presence of the holes in the hybrid joints does not lead to significant decrease of the stiffness respect to that of the simply bonded joint, whereas the load distribution between adhesive and rivets leads to significant advantages also in terms of energy absorption to failure; a significance synergism between the two coexistent junctions, rivets and adhesive, leads to an energy absorption to failure that is 2.0–2.5 times higher than that of simple joints, with a significant improvement of the damage tolerance.

In more detail, under static loading the two types of rivet, made by steel and aluminum, lead to comparable mechanical performances of the corresponding hybrid joints, although with very different damage mechanisms. Using aluminum rivets, the failure of the hybrid joint is due to the adhesive failure at the aluminum–composite interface, followed by the shear failure of the rivet. Using steel rivets, instead, the adhesive failure is followed by the rivet bending and the bearing failure of the CFRP, with subsequent final pull-out of the rivet.

In terms of fatigue strength, instead, the performance of the hybrid joint with steel rivets are better than those obtained with aluminum rivets, especially for high cycles fatigue.

In particular, for low cycles fatigue, the life of the hybrid joints with aluminum rivets increases by approximately 2–3 times compared to that of simply adhesively bonded joints, whereas for high cycles fatigue it tends to that of the simply adhesively bonded joints, without any appreciable improvement.

Unlike aluminum rivets, for both low and high cycles fatigue the hybrid joints with steel rivets exhibit a fatigue life of about 5–6 times that of the simply adhesively bonded joints.

Therefore, the work demonstrates that to obtain Al–CFRP hybrid joints with good mechanical performance, it is necessary to use steel rivets excluding the use of aluminum rivets, which also could cause corrosion phenomena between carbon and aluminum, especially near the hole edge where the carbon fibers may not be protected by the matrix.

Several numerical analyses carried out by using the ANSYS APDL environment with explicit solver, have shown that near the hole edges the riveting process can lead to local delamination of the CFRP adherents, especially between the two outer laminae.

The delamination is significantly more pronounced in the case of the steel rivet, and in the side of the rivet head where it reaches an extension equal to about the hole diameter (4–5 mm).

This initial delamination justifies the significant CFRP damage near the hole edge, experimentally observed both under static and fatigue loading conditions, especially for high cycles fatigue; in this case, in fact, there is a significant propagation of the delamination around the hole with subsequent pull-out of the rivet that precedes the final joint failure.

Therefore, further improvements of both the static and the fatigue strength of the hybrid joint with steel rivets, could be obtained by appropriate actions, as the use of special rivets with larger head and/or by adopting a higher clearance between the hole and the rivet itself, to avoid the successive growth of the initial delamination introduced by the riveting process near the CFRP hole edge.

References

[1] Kim Kwang-Soo, Yoo Jae-Seok, Yi Yeong-Moo, Kim Chun-Gon. Failure mode and strength of unidirectional composite single lap bonded joints. Compos Struct 2006;72:477–85.
[2] Owens James FP, Lee-Sullivan Pearl. Stiffness behaviour due to fracture in adhesively bonded composite-to aluminum joints. Int J Adhes Adhes 2000;20:39–45.
[3] Hart-Smith LJ. Adhesive-bonding double-lap joints. NASA CR-112235; 1973
[4] Choi Jin Ho, Lee Dai Gil. The torque transmission capabilities of the adhesively bonded tubular single lap joint and the double lap joint. J Adhes 1994;44:197–212.
[5] Moroni F, Pirondi A, Kleiner F. Experimental analysis and comparison of the strength of simple and hybrid structural joints. Int J Adhes Adhes 2010;30:367–79.
[6] Kelly Gordon. Quasi-static strength and fatigue life of hybrid (bonded/bolted) composite single-lap joints. Compos Struct 2006;72:119–29.
[7] Young-Hwan Lee, Do-Wan Lim, Jin-Ho Choi, Jin-HweKweon, Myung-Keun Yoon. Failure load evaluation and prediction of hybrid composite double lap joints. Compos Struct 2010;92:2916–26.
[8] da Silva Lucas FM, Pirondi A, Öchsner A, editors. Hybrid adhesive joints. Heidelberg: Springer; 2011.
[9] Hart-Smith LJ. Design methodology for bonded-bolted composite joints. Technical Report AFWAL-TR-81-3154, Douglas Aircraft Company; 1982.
[10] Hart-Smith LJ. Bonded-bolted composite joints. J Aircraft 1985;22:993–1000.
[11] Maofeng, Mallick PK. Fatigue of hybrid (adhesive/bolted) joints in SRIM. Int J Adhes Adhes 2001;21:145–59.
[12] Kelly G. Load transfer in hybrid (bonded/bolted) composite single-lap joints. Compos Struct 2005;69:35–43.
[13] Solmaz MY, Topkaya T. Progressive failure analysis in adhesively, riveted, and hybrid bonded double-lap joints. J Adhes 2013;89:822–36.
[14] Sadowski T, Knec M, Golewski P. Experimental investigations and numerical modeling of steel adhesive joints reinforced by rivets. Int J Adhes Adhes 2010;30:338–46.
[15] Ucsnik S, Scheerer M, Zaremba S, Pahr DH. Experimental investigation of a novel hybrid metal-composite joining technology. Compos A 2010;41:369–74.
[16] Kweon Jin-Hwe, Jung Jae-Woo, Kim Tae-Hwan, Choi Jin-Ho, Kim Dong-Hyun. Failure of carbon composite-to-aluminum joints with combined mechanical fastening and adhesive bonding. Compos Struct 2006;75:192–8.
[17] Russo A, Zuccarello B. Toward a design method for metal-composite co-cured joint based on the G-SIFs. Compos B Eng 2012;45(1):631–43.
[18] Di Franco G, Zuccarello B. Analysis and optimization of hybrid double lap aluminum–GFRP joints. Compos Struct 2014;116:682–93.
[19] Ascione L, Berardi VP, Feo L, Mancusi G. A numerical evaluation of the interlaminar stress state in externally FRP plated RC beams. Compos B Eng 2005;36(1):83–90.
[20] Ascione F. Mechanical behaviour of FRP adhesive joints: a theoretical model. Compos B Eng 2009;40(2):116–24.
[21] Ascione F, Feo L, Maceri F. On the pin-bearing failure load of GFRP bolted laminates: an experimental analysis on the influence of bolt diameter. Compos B Eng 2010;41(6):482–90.
[22] Ascione L, Feo L. Modeling of composite/concrete interface of RC beams strengthened with composite laminates. Compos B Eng 2000;31(6–7):535–40.
[23] Manes A, Giglio M, Viganò F. Effect of riveting process parameters on the local stress field of a T-joint. Int J Mech Sci 2011;53:1039–49.
[24] De Castro PMST, De Matos PFP, Moreira PMGP, Da Silva LFM. An overview on fatigue analysis of aeronautical structural details: open hole, single rivet lap-joint and lap-joint panel. Mater Sci Eng 2007;144:468–70.
[25] De Matos PFP, Moreira PMGP, Camanho PP, De Castro PMST. Numerical simulation of cold working of rivets holes. Finite Elem Anal Des 2005;41:989–1007.
[26] De Matos PFP, McEvily AJ, Moreira PMGP, De Castro PMST. Analysis of the effect of cold-working of rivet holes on the fatigue life of an aluminum alloy. Int J Fatigue 2007;29:575–86.
[27] MATES – Technical Data Sheet: Epoxy Resin I-SX10 ver2; 2013.
[28] ASTM D3039/D3039M. Standard test method for tensile properties of polymer matrix composite materials. ASTM International; 2008.
[29] Hart-Smith LJ. Adhesive-bonding double-lap joints. NASA CR-112235; 1973.
[30] Adams RD, Wake WC. Structural adhesive joints in engineering. Elsevier Applied Science Publishers; 1984.
[31] Matthews FL. Joining fibre-reinforced plastics. Elsevier Applied Science Publishers; 1987.
[32] Hoskin BC, Baker AA. Composite materials for aircraft structures. AIAA Education Series; 1986.
[33] Heslehurst RB. Design and analysis of structural joints with composite materials. USA: DESTech Publications; 1986.
[34] ASTM D3528–96. Standard test method for strength properties of double lap shear adhesive joints by tension loading; 2008
[35] Lucas FM, da Silva, Adams RD. Technique to reduce the peel stresses in adhesive joints with composites. Int J Adhes Adhes 2007;27:227–35. 2007.
[36] joints with composites, Int. Journal of Adhesion & Adhesives 2012;37:96–101. Crocombe AD, Richardson G. Assessing stress state and mean load effects on fatigue response of adhesively bonded joints. Int J Adhes Adhes 1999;19:19–27.
[37] Crocombe AD, Khoramishad H, Ashcroft, Katnam KB. A generalised damage model for constant amplitude fatigue loading of adhesively bonded joints. Int J Adhes 2010;30:513–21.
[38] Crocombe AD, Khoramishad H, Ashcroft, Katnam KB. Load ratio effect on the fatigue behaviour of adhesively bonded joints: an enhanced damage model. J Adhes 2010;86:257–72.
[39] Agarwal BD, Broutman LJ, Chandrashekhara K. Analysis and performance of fiber composites. 3rd ed. Wiley; 2006 (July).
[40] Barbero EJ. Introduction to composite materials design. 2nd ed. CRC Press; 2010 (July).